  Bull. Chem. Soc. Jpn., 62, 2781—2788 (1989)

Interactions of Excited Lithium Atom with Molecular Hydrogen. III. Orthogonality Constrained MCSCF+NCI Calculations of Potential Energy Surfaces and Electronic Wave Functions in the Potential Crossing Region

Masayuki TOYAMA,* Takayuki UCHIDE, Toshimasa YASUDA,§
Tokuo KASAI,§§ and Shiro MATSUMOTO
Department of Chemistry, College of Science and Engineering,
Aoyama Gakuin University, Chitosedai, Setagaya-ku, Tokyo 157
(Received January 30, 1989)

A method of calculating the excited state MCSCF electronic wave function by constraining it to be orthogonal to the predetermined ground state wave function was applied to calculate wave functions of the Li–H_2 system near the center of a conical intersection of the lowest two potential energy surfaces. Combined with an additional nonorthogonal configuration interaction process, it has proved to be an efficient method to get systems of wave functions that are continuous throughout whole geometries. Qualitative characters of wave functions near the center of potential crossing previously inferred have been reconfirmed.

Nonadiabatic transition is a key process to all physicochemical phenomena involving electronically excited states. It participates in every process where electronic energy is converted in to other kinds of energy. Its detailed mechanism, particularly how electrons will behave at the moment of transition, is of great theoretical interest.[1–9,18,35,37,38] Quenching of the fluorescence of alkali metal atoms by simple molecules is a prototype of relevant phenomena and suitable for detailed theoretical investigation, and has been the subject of many experimental and theoretical works.[10–43]

Many authors[25–28,41–43] have applied the classical trajectory method to potential energy surfaces calculated by some semiempirical methods. In those studies, discussion was often neglected on the nature of wave functions and detailed shapes of potential surfaces in the nonadiabatic region were often neglected. In ab initio calculation of wave functions[44,47–50,52,53] also, most concern has been given to detailed shapes of potential energy surfaces in their crossing regions and not to the nature of wave functions themselves.

For the Li–H_2 system, ab initio calculations of wave functions using large basis sets have been reported only for limited geometries.[34,36,38] Neither calculation of complete three-dimensional potential hypersurfaces nor analysis of wave functions near the center of their conical intersection[35] has hitherto been carried out by anyone including ourselves, despite their importance for detailed understanding of the nonadiabatic process. This is mainly because, as reported in the preceding paper,[54] direct MCSCF calculations of excited states for such geometries suffer convergence difficulties. Even if fortuitous convergence has been achieved, potential energy surfaces thus obtained often show apparent irregularities near crossing geometry, yielding electron density maps inadequate to excited states. Such cases have usually been treated by the state averaged MCSCF (SA-MCSCF) method.[44–53]† Using the method with weight factor 0.5 for lower accompanying states, we have obtained[54] smooth potential curves for the ground and excited states, but they lie somewhat higher than the corresponding curves obtained by the ordinary MCSCF method. Moreover, we have not been able to obtain SA-MCSCF functions if we use the weight factor 0.0 for lower states. This leaves some ambiguity in wave function obtained. To overcome these difficulties, we have introduced a new alternative method[54] to obtain excited MCSCF wave functions. It amounts to minimizing the energy requiring the function to be orthogonal[55] to a predetermined MCSCF ground state (hereafter, this method will be abbreviated as OC-MCSCF).

OC-MCSCF gives exactly the same function outside the crossing region as the conventional MCSCF method, and gives potential surfaces which seem to stand for smooth interpolations of potential surfaces obtained in the left and right sides of the crossing region, just as the SA-MCSCF method does, but energies are, in general, lower than those obtained by the SA-MCSCF method. The above-mentioned achievement of the present method has been gained by sacrificing, for general C_s geometries,[54] the generalized Brillouin theorem[56] to some extent. (SA-MCSCF functions with nonzero weight factors for lower accompanying states also may not fulfill the theorem.) Moreover, excited MCSCF function(s) in the potential crossing region may, in general, not be properly

§ Present address: Ashigara Research Laboratories, Fuji Photo Film Co., Ltd., Nakanuma, Minamiashigara, Kanagawa 250-01.

§§ Present address: Fujitsu Ltd., 3-21-8, Nishishinbashi, Minato-ku, Tokyo 105.

† Other methods of calculating correlated wave functions, such as Cluster Expansion Methods, CEPA, and MP2, are left aside here, and treatments in the MCSCF domain are discussed.

hamiltonian-orthogonal to the ground MCSCF function independently calculated for the same geometry. Thus, in our scheme,[54] a final nonorthogonal configuration interaction process (NCI) is taken from among all CSF's constituting the pair of ground and excited MCSCF functions. This guarantees the mutual orthogonality and hamiltonian-orthogonality of the final pair of MCSCF functions.

In this paper, we report the whole unified potential surfaces for the Li–H_2 system thus obtained. The nature of wave functions will also be discussed using suitable electron density maps.

Method of Calculation

The geometric parameters are shown in Fig. 1. The basis functions are the same as used in an earlier work.[38] Dill and Pople's 5-21G basis set was used for Li atom, and for H atoms the 4-31G basis set of Ditchfield et al.[58] was augmented by p-polarization functions of exponent 1.0 before use. All calculations were done with C_s symmetry of molecular orbitals. No further symmetry constraint was applied to orbitals even in higher symmetric geometries than C_{2v}. This was necessary to avoid any discontinuities in potential surfaces.[35,38] The selection of CSF was of CAS[59] type. The inactive space consisted of 1a′ orbital, and the active space consisted of (2a′—6a′) and 1a″ orbitals. Orbitals from 7a′ to 15a′ and 2a″, 3a″, and 4a″ were taken to be virtual. The resulting 45 CSF's corresponded to those of the minimal basis full valence calculation.

Ground state MCSCF functions were calculated by the standard one-step Newton–Raphson procedure using an exponetial formalism incorporated with a mode control and a mode damping process.[60] Near the center of the conical intersection of the ground and the excited state potential energy surface, each excited state wave function was calculated with a constraint of being orthogonal to the corresponding ground state wave function, by using a slight modification of the original MCSCF program, as reported in the preceding paper.[54] When the geometry was far from the critical geometry, both the constrained and the unconstrained program gave exactly the same result.

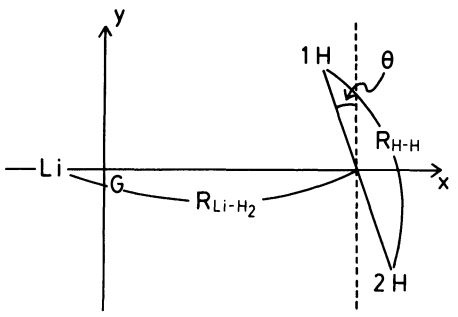

Fig. 1. Geometrical parameters for the Li–H_2 system.

In practice, we adopted the natural orbital expansion for all MCSCF functions to make their expressions unique since CAS wave function forms are invariant to any orbital rotations in the active space.

Then, we adopted the nonorthogonal configuration interaction for all CSF's (45×2=90 in all) constituting the primary pair of ground and excited MCSCF wave functions to get the final expression of states

$$\Psi = \sum_{i=1}^{N} A_i^{(G)} \Phi_i^{(G)} + \sum_{i=1}^{N} A_i^{(E)} \Phi_i^{(E)},$$

where $\Phi_i^{(G)}$'s are the CSF's obtained for the ground MCSCF function, and $\Phi_i^{(E)}$'s are those for the excited MCSCF function. $A_i^{(G)}$'s and $A_i^{(E)}$'s are taken freely to make $\langle \Psi | H | \Psi \rangle$ stationary under a sole condition of $\langle \Psi | \Psi \rangle = 1$.

Results and Discussion

1 C_{2v} Geometry. (1) Potential Energy Curves in the Immediate Neighborhood of the Center of Intersection: Figure 2 shows the total energies of the system calculated by the method described above along some reaction coordinate defined earlier[38] on the C_{2v} potential energy surface. The solid lines show the results before NCI and the chain lines show those after NCI. The ground state energies (filled circles in Fig. 2) were obtained directly by the usual MCSCF method,

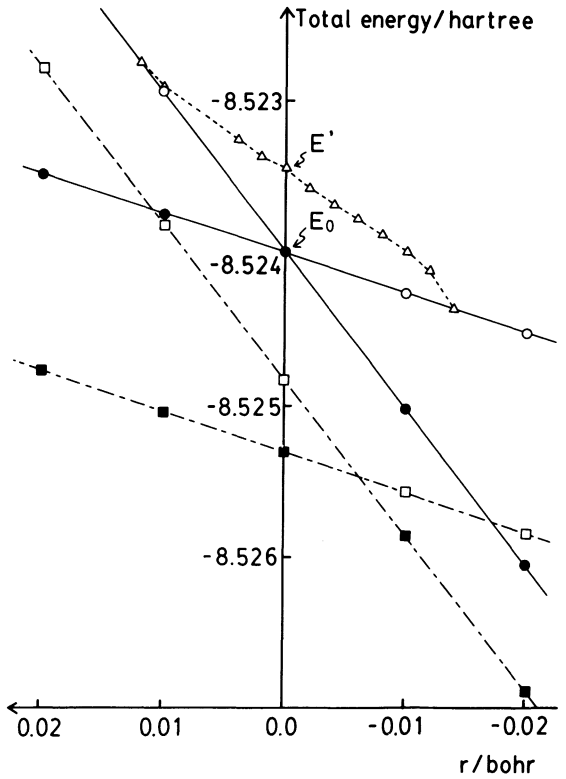

Fig. 2. Comparison of potential energy curves near the point P along the reaction coordinate r calculated by conventional MCSCF: (●, △), OC-MCSCF: (○), OC-MCSCF+NCI: (■, □).

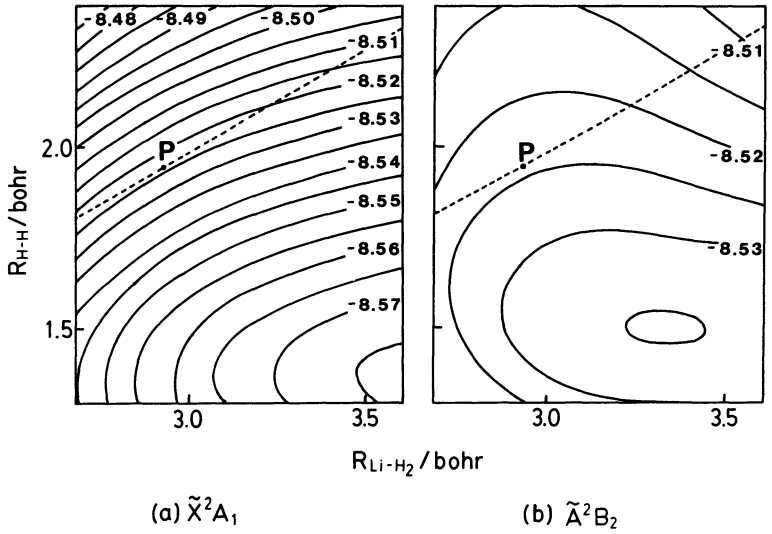

Fig. 3. Contour plots of the two lowest potential energy surfaces near their crossing seam (broken lines). Energies are given in hartrees. *P* is the lowest point on the crossing seam.

while the excited state energies (open circles in Fig. 2) were obtained by OC-MCSCF using the corresponding ground state as reference. As seen in the figure, no irregularities occur in the OC-MCSCF curve as is usually reported in SA-MCSCF calculations.[44,48–50,52,53]†† The open triangles in the figure indicate energies of excited states when the constraint was not applied. When the geometry was relatively far from the *P* point, i.e., $r \gtrsim 0.01$ or $r \lesssim -0.015$ bohr, open triangles fell on the open circles, and the wave functions with and without constraint were identical after the MO's were transformed to natural orbitals. As we see from the 3a′ natural orbital electron density maps in Figs. 5(a) and (b), for example at $r=0$, the symmetry of the wave functions by the method are correctly of C_{2v}, even though no C_{2v} constraint was put on the MO form. The typical energy lowering by the NCI was 7×10^{-4} hartree at the *P* point. For further details see Ref. 54.

(2) C_{2v} Potential Energy Surfaces in the Crossing Region: Figure 3 shows the lowest two potential energy surface contour maps thus obtained for a wider range of geometries around the central point of the crossing region. The broken lines indicate the crossing seam between the surfaces. The location and energy of the *P* point (the lowest point on the seam) are $R_{Li-H_2}=2.9344$ and $R_{H-H}=1.9520$ bohr, respectively. It lies 1.1×10^{-3} hartree lower than the energy of $Li(^2P)+H_2(^1\Sigma_g^+)$. The depth of the pond on the excited state potential surface is 1.26×10^{-2} hartree, and its bottom is located at ($R_{Li-H_2}=3.35$, $R_{H-H}=1.55$ bohr). These values deviate somewhat from the values of Hobza and Schleyer.[34] The difference may be due mainly to the basis set quality, but may also have resulted from the small NCI size adopted in the work. Even the size of the wave function set used in the present NCI may be sufficient in improving both qualities and some of the energies of MCSCF functions in the vicinity of the potential crossing center, but for other geometries it is rather insufficient. Increasing the size of NCI would have no difficulty and may improve the whole of the unified potential surfaces. The results will be reported in future papers. The main additional task in OC-MCSCF plus NCI procedure over the usual MCSCF procedure is the construction of second order transition density matrix elements between the ground and the excited state. This did not cause any methodological difficulties, but required about 20% extra CPU time over the ordinary procedure in iterations.

It should be noted that we have found a small dip in the C_{2v} ground state potential energy surface. It is located at ($R_{Li-H_2}=11.8$, $R_{H-H}=1.4$ bohr) and has a depth of 8.2 μhartree. It probably corresponds to the van der Waals interaction of $Li(^2S)$ and $H_2(^1\Sigma_g^+)$. A minimum also is observed in our $C_{\infty v}$ calculations at ($R_{Li-H_2}=12.3$, $R_{H-H}=1.4$ bohr), and its depth is 5.2 μhartree. Hobza and Schleyer[34] also reported a minimum on their potential energy surface for $C_{\infty v}$ symmetry ($R_{Li-H_2}=11.4$, $R_{H-H}=1.4$ bohr, 30 μhartree†††).

2 C_s Geometry. The OC-MCSCF method was most effective in computing the excited states in C_s geometries. Figure 4 shows part of the various poten-

†† In this case also, we got smooth SA curves some 5×10^{-3} hartree shifted upwards relative to the OC-MCSCF excited and ground state curves. (cf. Ref. 54)

††† Referring to Table 1 of Ref. 34, we obtain the numerical value for the depth given above, instead of "13 kcal mol^{-1}" given in the text of that paper.

tial curves obtained by three methods, conventional MCSCF, OC-MCSCF, and OC-MCSCF+NCI, when the H_2 molecule was rotated from the C_{2v} geometry of the point P with $R_{Li\text{-}H_2}$ and $R_{H\text{-}H}$ kept fixed. The actual calculation was started from $\theta=90°$ ($C_{\infty v}$) and proceeded step by step down to $\theta=0°$ by using the converged MC function at a previous geometry as the 0th approximation of iteration. The OC-MCSCF function at $\theta=90°$ was obtained from the function at ($R_{Li\text{-}H_2}=3.0$, $R_{H\text{-}H}=1.4$ bohr, $\theta=90°$), the latter function being calculated in the opposite direction, i.e., by starting from ($R_{Li\text{-}H_2}=3.0$, $R_{H\text{-}H}=1.4$ bohr, $\theta=0°$, C_{2v}) and increasing θ up to 90°. At the last geometry, there was no ambiguity in identifying the ground and excited state MCSCF functions since they are sufficiently outside the geometric region where the usual MCSCF procedure shows irregularities.

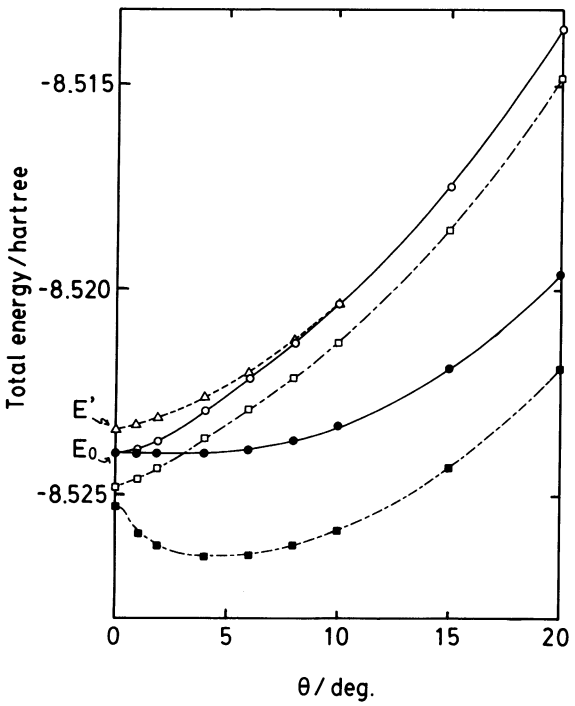

Fig. 4. Potential energy curves of the ground state and the first excited state vs. rotation angle θ from the C_{2v} geometry at point P. $R_{Li\text{-}H_2}$ and $R_{H\text{-}H}$ are fixed constant. Conventional MCSCF: (●, Δ), OC-MCSCF: (○), OC-MCSCF+NCI: (■, □).

In Fig. 4, as θ decreases from 20°, the MCSCF excited state curve deviates upward from the OC-MCSCF curve and reaches the energy E', somewhat higher than that of the MCSCF ground state at $\theta=0°$ (E_0). The energy E' is equal to the energy of the excited state obtained by an MCSCF calculation on C_{2v} geometries (E' in Fig. 2). An electron density map analysis also has shown that the MCSCF excited state thus obtained has no correct C_{2v} symmetry. These reveal the inadequateness of the conventional MCSCF method for the central portion of potential crossing geometries. (We have made many other attempts by starting with different 0th approximations or using different algorithms, but none of them has been successful.) On the other hand, the OC-MCSCF curve reaches E_0 just at $\theta=0°$ and there occur no discontinuities between the C_{2v} and C_s potentials. After the MO's were converted to natural orbitals, the OC-MCSCF function at $\theta=0°$ was identical with that obtained in section 1-(1). The 3a′

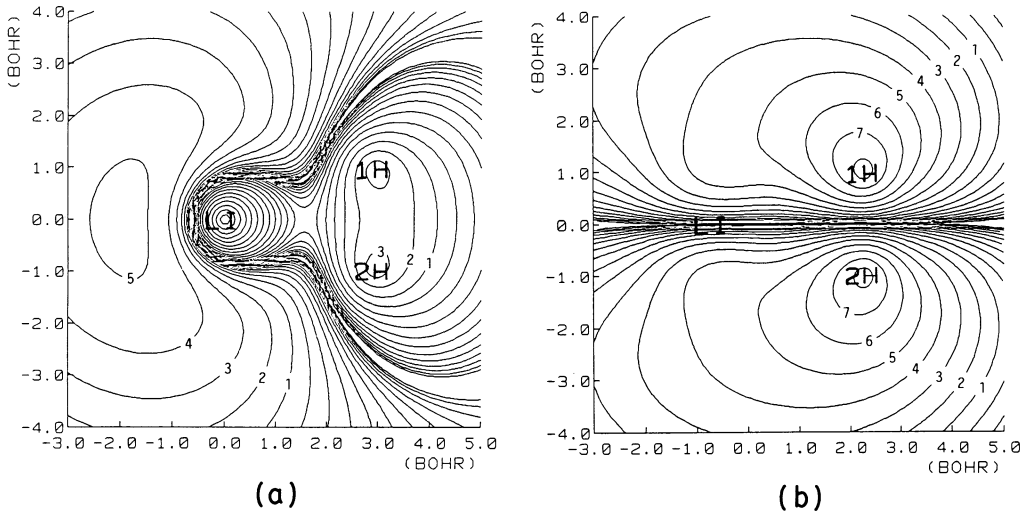

Fig. 5. Contour plots of 3a′ natural orbital electron density maps at P (a) the $\tilde{X}^2A_1$ state obtained by conventional MCSCF and (b) $\tilde{A}^2B_2$ state obtained by OC-MCSCF. The numbers 1, 2, ⋯, and 7 beside the contours indicate electron density of 6.325×10^{-4}, 1.125×10^{-3}, 2.000×10^{-3}, 3.556×10^{-3}, 6.325×10^{-3}, 1.125×10^{-2}, 2.000×10^{-2} electrons bohr^{-3}, respectively.

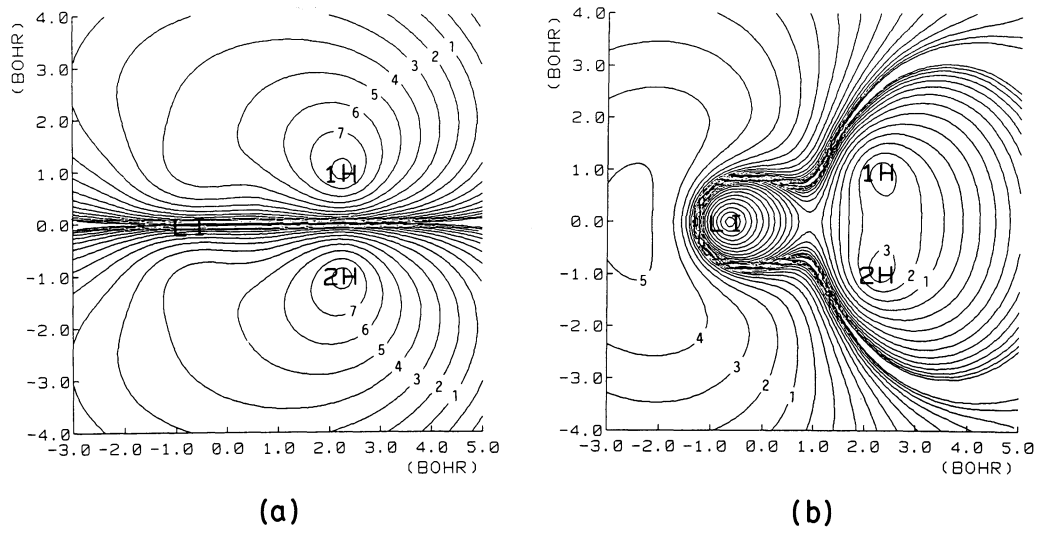

Fig. 6. Similar maps as in Fig. 5, after NCI.

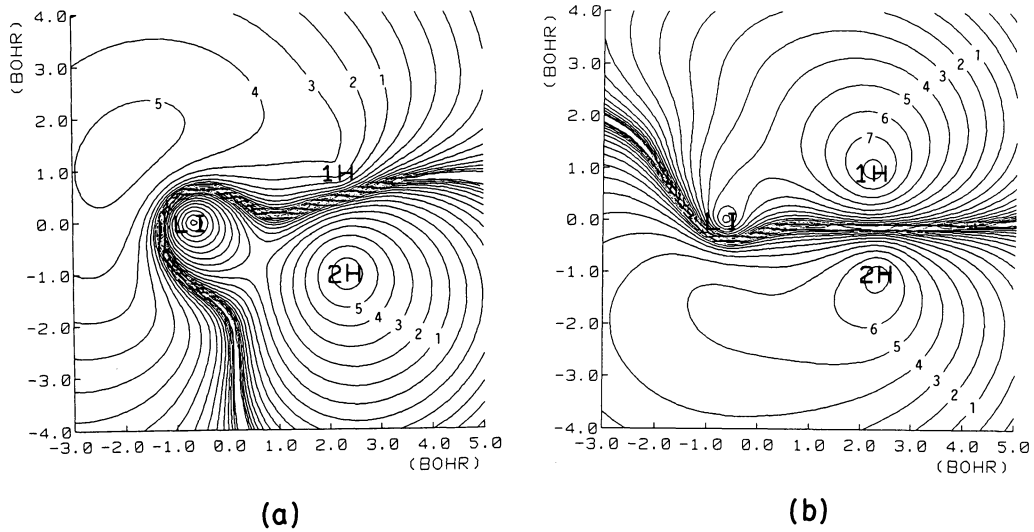

Fig. 7. Contour plots of 3a′ natural orbital electron density maps at a geometry where H_2 is rotated 4.0° from the geometry of P with $R_{Li\text{-}H_2}$ and $R_{H\text{-}H}$. (a) the $1^2A'$ state obtained by conventional MCSCF and (b) $2^2A'$ state obtained by OC-MCSCF. Figures besides contours have the same meaning as in Fig. 6.

natural orbital electron density maps of the ground and excited states are thus identical with Figs. 5(a) and (b), which show the correct symmetry of the functions.

As seen in Fig. 4, the NCI splits the energies of the almost degenerate OC-MCSCF function pair at $\theta=0°$. As a consequence, the intersection of the $^2A_1$ and $^2B_2$ curves in C_{2v} geometry shifts somewhat, as seen in Fig. 2. At the same time, we get small but definite energy improvements (cf. section 1-(1)) at the geometry.

Common to all results reported hitherto,[35,37,38] there is a minimum (at $\theta=5°$ with a depth of 4.4×10^{-3} hartree relative to $\theta=0°$) in the ground state curve, while the excited state curve increases monotonically as θ increases.

Figures 6(a) and (b) are the 3a′ natural orbital electron density maps of the pair states at $\theta=0°$ after NCI. They also show C_{2v} symmetry.†††† Figures 7(a) and (b) show similar density maps taken at $\theta=4.0°$ before NCI. It is seen that both the functions have their own unique natures widely differing from each other. It is a favorable feature for them to be the basis of the succeeding NCI step since as we are inclined to gather a maximum degree of information from the

†††† The interchange between the $^2A_1$ and $^2B_2$ state energies is due to the shift of the P point noted above.

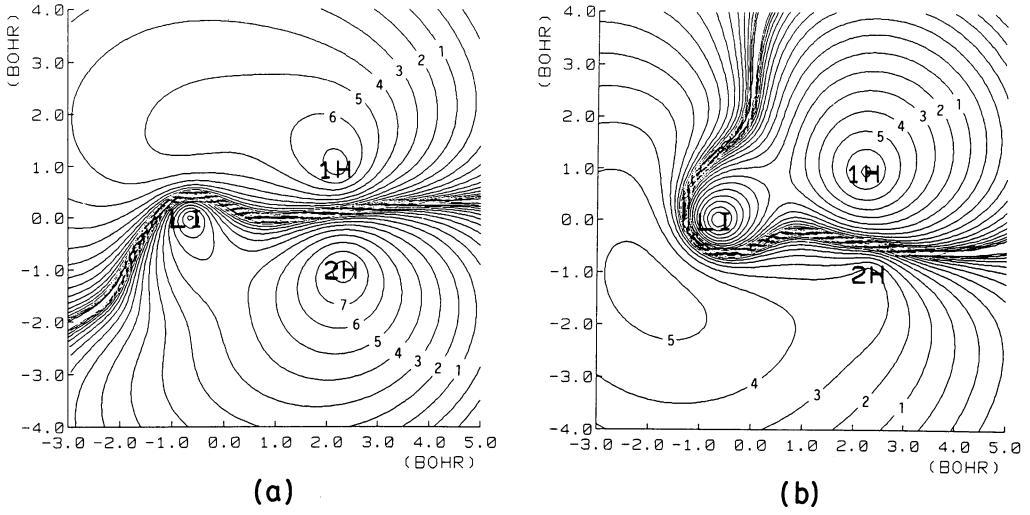

Fig. 8. Similar maps as in Fig. 7, after NCI.

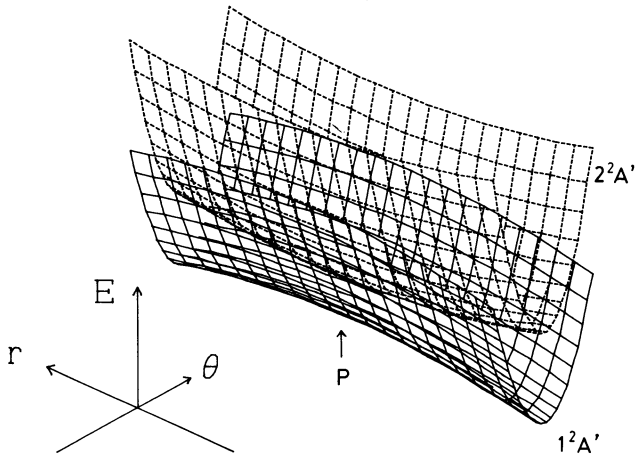

Fig. 9. Computer graphical representation of the $1^2A'$ and $2^2A'$ adiabatic potential energy surfaces in θ and r dimensions near the apex of the conical intersection.

primary MCSCF function of limited size to construct final functions. In this connection, Hosteny and Hagstrom[61] and Petsalakis et al.[62,63] have argued that the effect of NCI may be comparable to that of an ordinary large size CI when the two sets of CSF's differ considerably. Figures 8(a) and (b) are the maps after the NCI. The improvement by NCI of the main features of these maps had turned out not to be very significant,†††† and the features of the final function are in good agreement with those reported earlier for less quantitative calculations (minimal basis valence CAS,[33,35] minimal basis full CI,[37] and SCF+NCI[38] using the same basis set as the present one) with respect to the bonding nature of the shorter Li–H in the ground state and the bonding nature of the longer Li–H in the excited state.

In order to obtain certain cross sections of the three dimensional hypersurfaces, we carried out similar calculations starting with many geometries for the reaction coordinate of section 1-(1). Using some interpolation techniques, these results were combined to give two sheets of potential energy surfaces. Figure 9 is a computer graphical representation of these surfaces. The outlook of these surfaces is very much the same as reported earlier,[35] but it is now more quantitative.

Conclusion

In summary, the OC-MCSCF and the additional NCI procedure described in this and the preceding paper provide an effective means of constructing excited state MCSCF functions and of the corresponding ground state functions in geometries where their potential energy surface fall close to each other or even cross with each other. The potential energy surfaces and the functions themselves connect continuously with the ones calculated by the ordinary MCSCF procedure outside the critical region, and no discontinuities occur between them. The excited state function is strictly orthogonal and hamiltonian orthogonal to its corresponding ground state function. The method is general, and only a little extra work over the ordinary method is required in constructing the second order transition density matrix. Further, by extension of the size of NCI, the method may give us unified MCSCF functions and potential surfaces which are good throughout a wide range of geometries, not restricted to the nonadiabatic region. The geometrical symmetries of the wave functions tested for the present special case seem to be reasonable.

Conclusions reported in earlier papers concerning

†††† The apparent interchange between the characteristics of $1^2A'$ and $2^2A'$ maps is for the same reason as given in the footnote.††††

the behavior of wave functions of the Li-H_2 system in the nonadiabaic region have been reconfirmed in the present more quantitative calculations.

The authors wish to thank Professor Keiji Morokuma of the Institute for Molecular Science and Dr. Shigeki Kato of the University of Tokyo. The calculations were carried out at the Computer Center of the IMS, Okazaki National Research Institutes, at the Computer Center of the University of Tokyo, and at the Information Science Research Center of Aoyama Gakuin University.

References

1) M. Desouter-Lecomte, C. Galloy, J. C. Lorquet, and M. Vaz Pires, *J. Chem. Phys.*, **71**, 3661 (1979), and the preceding papers by the same authors. See also references cited therein.
2) D. Dehareng, X. Chapuisat, J. C. Lorquet, C. Galloy, and G. Rassev, *J. Chem. Phys.*, **78**, 1246 (1983).
3) M. Desouter-Lecomte, D. Dehareng, B. Lehy-Nihant, M. Th. Praet, A. J. Lorquet, and J. C. Lorquet, *J. Phys. Chem.*, **89**, 214 (1985).
4) R. D. Levine, *Bull. Chem. Soc. Jpn.*, **61**, 29 (1988).
5) B. C. Garrett, M. J. Redmon, D. G. Truhlar, and C. F. Melius, *J. Chem. Phys.*, **74**, 412 (1981).
6) B. C. Garrett, D. C. Truhlar, and C. F. Melius, *Phys. Rev. A*, **24**, 2853 (1981).
7) S. Kato, R. L. Jaffe, A. Komornicki, and K. Morokuma, *J. Chem. Phys.*, **78**, 4567 (1983).
8) M. Baer, I. Last, and Y. Shima, *Chem. Phys. Lett.*, **110**, 163 (1984).
9) C. Leforestier, *Chem. Phys. Lett.*, **125**, 373 (1986).
10) J. L. Magee and T. Ri, *J. Chem. Phys.*, **9**, 638 (1941).
11) K. J. Laidler, *J. Chem. Phys.*, **10**, 34 (1942).
12) G. J. Schulz, *Rev. Mod. Phys.*, **45**, 422 (1973).
13) J. R. Barker and R. E. Weston Jr., *J. Chem. Phys.*, **45**, 1427 (1976).
14) I. V. Hertel, H. Hofmann, and K. A. Rost, *Chem. Phys. Lett.*, **47**, 163 (1977).
15) A. Sevin and P. Chaquin, *Chem. Phys.*, **93**, 49 (1985).
16) C. Crepin, J. L. Picque, G. Rahmat, J. Verges, R. Vetter, F. X. Gadea, M. Pelissier, F. Spiegelmann, and J. P. Malrieu, *Chem. Phys. Lett.*, **110**, 395 (1984).
17) P. Herbitz, *Chem. Phys.*, **54**, 131 (1980).
18) P. Botschwina, W. Meyer, I. V. Herterl, and W. Reiland, *J. Chem. Phys.*, **75**, 5438 (1981).
19) D. Papierowska-Kaminski, M. Persico, and V. Bonačić-Koutecký, *Chem. Phys. Lett.*, **113**, 264 (1985).
20) A. Sevin and P. Chaquin, *Chem. Phys.*, **93**, 49 (1985).
21) D. R. Yarkony, *J. Chem. Phys.*, **84**, 3206 (1986).
22) A. Sevin, P. C. Hiberty, and J.-M. Lefour, *J. Chem. Phys.*, **109**, 1845 (1987).
23) D. Poppe, D. Papierowska-Kaminski, and Bonačić-Koutecký, *J. Chem. Phys.*, **86**, 822 (1987).
24) M. M. Gallo and D. R. Yarkony, *J. Chem. Phys.*, **86**, 4990 (1987).
25) D. G. Truhlar, J. W. Duff, N. C. Blais, J. C. Tully, and B. C. Garrett, *J. Chem. Phys.*, **77**, 764 (1982).
26) N. C. Blais and D. G. Truhlar, *J. Chem. Phys.*, **79**, 1334 (1983).
27) N. C. Blais, D. G. Truhlar, and B. C. Garrett, *J. Chem. Phys.*, **78**, 2956 (1983).
28) C. W. Eaker, *J. Chem. Phys.*, **87**, 4532 (1987).
29) D. R. Jenkins, *Proc. R. Soc. London, Ser. A*, **306**, 413 (1968).
30) J. Elward-Berry and J. E. Berry, *J. Chem. Phys.*, **72**, 4510 (1980).
31) C. H. Meller III, K. Schofield, and M. Steinberg, *J. Chem. Phys.*, **72**, 6620 (1980).
32) J. Derouard and N. Sadeghi, *Chem. Phys. Lett.*, **111**, 353 (1984).
33) K. Mizutani, Y. Kuribara, K. Hayashi, and S. Matsumoto, *Bull. Chem. Soc. Jpn.*, **52**, 2184 (1979).
34) P. Hobza and P. R. Schleyer, *Chem. Phys. Lett.*, **105**, 630 (1980).
35) K. Mizutani, T. Yano, A. Sekiguchi, K. Hayashi, and S. Matsumoto, *Bull. Chem. Soc. Jpn.*, **57**, 3368 (1984).
36) J. García-Prieto, W. L. Feng, and O. Novaro, *Chem. Phys. Lett.*, **119**, 128 (1985).
37) K. Mizutani, M. Toyama, K. Taguchi, and S. Matsumoto, *Comput. Chem.*, **9**, 259 (1985).
38) S. Matsumoto, K. Mizutani, A. Sekiguchi, T. Yano, and M. Toyama, *Int. J. Quantum Chem.*, **29**, 689 (1986).
39) P. Saxe and D. R. Yarkony, *J. Chem. Phys.*, **86**, 321 (1987).
40) A. Sevin, P. Chaquin, L. Hamon, and P. C. Hiberty, *J. Phys. Chem.*, **110**, 5681 (1988).
41) J. C. Tully, *J. Chem. Phys.*, **59**, 5122 (1973).
42) C. W. Eaker, *J. Phys. Chem.*, **92**, 3858 (1988).
43) J. C. Tully, "Dynamics of Molecular Collisions," ed by W. H. Miller, Plenum, New York (1976), Part B, pp. 217—267.
44) K. Docken and J. Hinze, *J. Chem. Phys.*, **57**, 4928 (1972).
45) J. Hinze, *J. Chem. Phys.*, **59**, 6424 (1973).
46) C. C. J. Roothaan, J. H. Detrich, and D. G. Hopper, *Int. J. Quantum Chem.*, **S13**, 93 (1979).
47) K. Rudenberg, L. M. Cheung, and S. T. Elbert, *Int. J. Quantum Chem.*, **16**, 1069 (1979).
48) H.-J. Werner and W. Meyer, *J. Chem. Phys.*, **74**, 5794 (1981).
49) R. N. Differnderfer and D. R. Yarkony, *J. Phys. Chem.*, **86**, 5098 (1982).
50) B. Pouilly, B. H. Lengsfield, and D. R. Yarkony, *J. Chem. Phys.*, **80**, 5089 (1984).
51) H.-J. Werner, "Ab Initio Methods in Quantum Chemistry," ed by K. P. Lawley, Wiley, New York (1987), Vol. LXIX, Part II, pp. 1—62.
52) P. Saxe, B. H. Lengsfield III, and D. R. Yarkony, *Chem. Phys. Lett.*, **113**, 159 (1985).
53) M. I. McCarthy, P. Rosmus, H.-J. Werner, P. Botschwina, and V. Vaida, *J. Chem. Phys.*, **86**, 6693 (1987).
54) S. Matsumoto, M. Toyama, T. Yasuda, T. Uchide, and R. Ueno, *Chem. Phys. Lett.*, in Press.
55) H. G. Miller and R. M. Dreizler, *Nucl. Phys. A*, **316**, 32 (1979).
56) A. C. Wahl and G. Das, "Methods of Electronic Structure Theory," ed by H. F. Schaefer III, Plenum, New York (1977), Vol. III, pp. 51—78.
57) J. D. Dill and J. A. Pople, *J. Chem. Phys.*, **62**, 2921 (1975).

58) R. Ditchfield, W. J. Hehre, and J. A. Pople, *J. Chem. Phys.*, **54**, 724 (1971).
59) B. O. Roos, "Methods in Computational Molecular Physics," ed by G. H. F. Diercksen and S. Wilson, D. Reidel Publishing Company, Dordrecht (1983), NATO ASI Series C, Vol. 113, pp. 161—187.
60) J. Olsen, D. L. Yeager, and F. Jørgensen, "Advances in Chemical Physics," ed by I. Prigogine and S. A. Rice, Wiley, New York (1985), Vol. LIV, pp. 1—176.
61) R. P. Hosteny and S. A. Hagstrom, *J. Chem. Phys.*, **58**, 4396 (1973).
62) I. D. Petsalakis, G. Theodorakopoulos, C. A. Nicolaides, R. J. Bunker, and S. D. Peyerinhoff, *J. Chem. Phys.*, **81**, 3161 (1984).
63) I. D. Petsalakis, G. Theodorakopoulos, C. A. Nicolaides, and R. J. Bunker, *J. Chem. Phys.*, **81**, 5952 (1984).